Carbohydrate Research, 220 (1991) 33–47
Elsevier Science Publishers B.V., Amsterdam

Physico-chemical properties of aqueous solutions of xanthan: An n.m.r. study

Amelia Gamini*, Jan de Bleijser, and Jaap C. Leyte†
Department of Physical and Macromolecular Chemistry, Gorlaeus Laboratory, Leiden Univeristy, P.O. Box 9502, 2300 RA Leiden (The Netherlands)

(Received October 10th, 1990; accepted for publication March 30th, 1991)

ABSTRACT

The conformations of xanthan in aqueous solution as a function of temperature have been studied. Measurements of optical activity indicate that the conformational transition, induced by varying the polymer concentration, is analogous to that induced by changes in ionic strength and pH. Within a certain range of concentrations, the low-temperature conformation has a molecular-weight-dependent stability, which shows the usual sigmoidal melting profile with increase of temperature. The ^{13}C-n.m.r. data reflect the increase of the mobility of C-1 and the side-chain carbon atoms in the transition-temperature region. The ^{23}Na relaxation behaviour changes on melting the ordered xanthan conformation. At least two correlation times are needed in order to describe the field-strength dependence of the longitudinal and transverse ^{23}Na relaxation. At 25°, a value of 6.8 ns is obtained for the largest correlation time for the fluctuations of the electric-field gradient. The high-temperature conformation also generates correlation times of the order of ns. From ^{17}O relaxation measurements, a reduction of the mobility of water molecules in the presence of xanthan chains is also observed.

INTRODUCTION

Xanthan gum, an extracellular polysaccharide produced by fermentation by the bacterium *Xanthomonas campestris*, forms highly viscous and pseudoplastic solutions[1,2] at relatively low concentrations, which have important industrial applications, particularly in oil recovery and in the food industries[3]. Xanthan consists[4] of a pentasaccharide repeating unit (**1**) with a (1→4)-β-D-glucopyranan (cellulosic) backbone with *O*-β-D-mannopyranosyl-(1→4)-*O*-β-D-glucopyranosyluronic acid-(1→2)-6-*O*-acetyl-α-D-mannopyranosyl side chains 3-linked to alternate glucose residues. A pyruvic acetal substituent is present on the terminal mannose residue to an extent that depends on the strain of bacteria, the conditions of fermentation and, probably, the purification procedures.

* Present address: Department of Biochemistry, Biophysics and Macromolecular Chemistry, University of Trieste, Trieste, Italy.
† To whom correspondence should be addressed.

0008-6215/91/$ 03.50

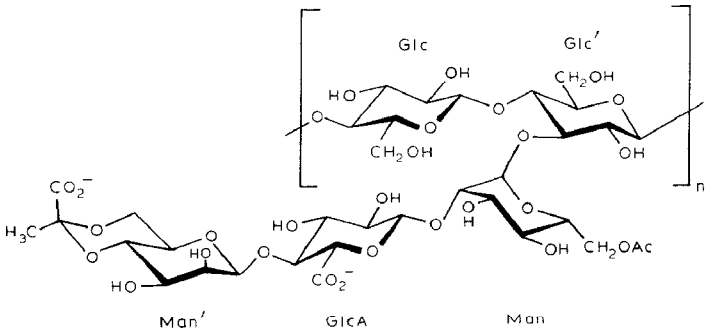

1

There is still a question as to whether xanthan exists as a single or dimeric structure, and it is well known that a conformational transition occurs with changes in ionic strength, pH, and temperature[5-8]. This transition depends also on the degree of substitution (d.s.) by pyruvic and acetyl groups.

Such a conformational transition has been detected by changes in specific optical activity, circular dichroism (c.d.), and by viscosity, calorimetric, and ^{1}H-n.m.r. measurements[5-9]. This experimental evidence has been interpreted in terms of an ordered-to-disordered transition, where the ordered state is stabilised by low temperatures and high ionic strengths.

Despite these extensive investigations, neither the ordered nor the disordered structure of xanthan chains in aqueous solution have a clear and generally accepted description. The dependence of the optical activity on ionic strength and on temperature has been used as experimental support for both single[10,11] and dimer[12,13] models. In the single chain model, the ordered structure is assumed to be a single helix, stabilised by low temperatures and high ionic strengths, and the transition was depicted as a single helix-to-coil transition. For the double-stranded helix model, the temperature-induced conformational transition has been interpreted as the change from a double helix to a dimerised expanded coil which partly retains double-helix fragments[12,14,15]. The latter interpretation was needed to account for the invariability of the molecular weight of samples of xanthan with temperature even above the conformational melting region[12].

A different interpretation of the conformational transition has been suggested in terms of ordered structures that are stabilised by interactions of the side chains and the backbone[16]. The contribution of the side chains to the optical activity has been suggested to change with increase in the ionic strength[11].

However, most of the authors seem inclined to accept the dimer as the most likely secondary structure in the ordered state for native xanthan[12-15,17-21] even though further inter-chain association was not excluded[21].

The work now reported was undertaken to acquire more information on the temperature-induced conformational change. Since no clear picture exists of the ordered state of xanthan, the temperature-induced conformational transition is discussed in general terms through changes of the physical properties of the ionic polysaccharide molecules. The results discussed here comprise ^{13}C-n.m.r. spectra and $^{23}Na^+$ relaxation

times obtained for salt-free solutions of sonicated samples of xanthan as a function of temperature.

N.m.r. spectroscopy is a powerful tool in studies of the properties of polyelectrolyte solutions[22–31] and ^{13}C relaxation yields information on the dynamics of the macromolecules. However, in the ordered conformation, the mobility of xanthan is so low that the ^{13}C-n.m.r. spectra cannot be resolved because of the large line-width. During the conformational transition, the mobility increases and the lines narrow. Assuming that the line shape does not change during the transition, then the peak heights are a measure of T_2. Therefore, this transition can be monitored by the amplitudes of the lines as a function of temperature. Whereas detailed relaxation studies will be needed in due course, the present naive approach is sufficient since the difference in behaviour between the main chain and the side chains in the premelting range can be observed clearly.

A detailed study of the relaxation processes will be extremely time consuming because of the low concentration (~0.03M) necessary to prevent the formation of microgels, and will have to be performed at several field strengths, since more than one correlation time will be involved for many lines.

Quadrupolar relaxation measurement is often applied in the study of ion–polymer interactions in both synthetic and biological systems[22,23,25–31]. Quadrupolar nuclei, *e.g.*, ^{23}Na, are especially suited for the study of polyelectrolytes because their relaxation is driven by fluctuating electric-field gradients at the site of the nucleus. These gradients arise from the surrounding water molecules and neighbouring polyelectrolyte molecules. Therefore, in favorable situations, it is possible to obtain correlation times of local motions of the field gradients by studying the quadrupolar relaxation of suitable counter-ions.

^{17}O relaxation measurements are useful in studies of the rotational dynamics of water, since the longitudinal relaxation is completely intramolecular. Furthermore, only a small isotopic enrichment is necessary in order to obtain an adequate S/N ratio.

EXPERIMENTAL

Preparation and purification of sonicated samples of xanthan. — A food-grade Keltrol T (Kelco) xanthan was used. All other chemicals were analytical grade. Deionised water was obtained using a Milli-Q (Millipore) purification system.

NaCl was added to 0.5M to ~5.3×10^{-3} monomol/L xanthan and a first precipitation by ethanol (30% vol.) was effected. The precipitate was recovered by filtration, and a solution in 0.1M NaCl was sonicated under N_2 at 175 W using a W 370 sonicator (Heat-Systems-Ultrasonics Inc.) with a 0.75-in. diam. macrotip. In order to prevent contamination by titanium ions, the tip was covered by a sapphire plate. During the degradation process, the temperature was maintained at 5°.

Three samples (FS1–3) were obtained after sonication for 1, 5, and 15 h, respectively. Each product was precipitated by ethanol or acetone, redissolved in 0.5M NaCl, and fractionated by acetone–water mixtures[17]. The central fraction of each of the 3 or 5

fractions obtained was then dissolved in 0.5M NaCl, the solution was dialysed against EDTA, EGTA, and finally against deionised water until the conductance of the external dialysis bath reached the value of deionised water ($7 \times 10^{-7}\Omega^{-1}$ cm^{-1}). Part of each solution was stored at $-20°$ after the addition of a trace of sodium azide, and the remainder was freeze-dried. The dry polymer was used for the preparation of samples for n.m.r. and optical activity studies. The stock solutions were used for light scattering, $\delta n/\delta c$, and $[\alpha]_{365}$ measurements.

The concentrations of the stock solutions were determined by freeze-drying a known amount of solution. The weight of the dry polymer was corrected for the water content as determined by the Karl-Fischer method.

Optical activity. — Specific optical activities were determined at 365 nm with a Perkin–Elmer 241 Spectropolarimeter equipped with a thermostated quartz cell of 1- or 0.1-dm path length.

Potentiometry. — Potentiometric titrations were performed using Radiometer equipment (TTT80 titrator, ABU80 Autoburette, PHM82 Standard pH meter, and REC80 Servograph). Samples of xanthan in the H^+ form were obtained by dialysing stock solutions against 0.1M HCl for ~24 h. The excess ions were removed by exhaustive dialysis against deionised water. The pH of the solutions was in the range 2.8–3.2. The mean equiv. wt. of each xanthan fraction is given in Table I.

Polymer concentrations were determined by freeze-drying as described above.

^{1}H-n.m.r. spectroscopy. — In order to determine the d.s. by acetal and pyruvate groups, ^{1}H-n.m.r. spectra (internal hydroquinone[32]) were obtained at 90°, using a Jeol JNM-FX-200 spectrometer; 200 scans, on average, were accumulated with a repetition time of 3 s and a spectral width of 3 kHz. Each sample of xanthan was exchanged three times with D_2O by freeze-drying, then dissolved in a weighed amount of D_2O (99.8%). A freshly prepared solution of hydroquinone in D_2O was added in order to obtain equimolar concentrations (expressed as monomol/L) of hydroquinone and polymer.

^{13}C-N.m.r. spectroscopy. — ^{13}C-N.m.r. spectra (100 MHz) were obtained on 2.6×10^{-2} monomol/L solutions of xanthan (FS3) in D_2O, using a Bruker MSL 400 spectrometer. Spectra in the range 40–90° were obtained by accumulating 10,000 scans with a repetition time of 0.8 s, using a 25-kHz spectral width. A line broadening of 50 Hz was

TABLE I

Molecular characterisation of xanthan samples

Sample	$M_w \times 10^{5a}$	*Equiv. wt*	$D.s._{Pyr}{}^b$	$D.s._{Ac}{}^c$
FS1	18.0 ±0.4	623 ±10	0.5 (0.5)[d]	1.0
FS2	5.4 ±0.2	629 ±3	0.5 (0.49)	1.0
FS3	2.3 ±0.1	626 ±10	0.47 (0.49)	0.9

[a] From low-angle laser-light scattering on solutions in 0.1M NaCl. [b] Number of pyruvate groups per repeating unit, determined by ^{1}H-n.m.r. spectroscopy at 90°. [c] Number of acetate groups per repeating unit. [d] Values in brackets were determined by potentiometric titration at room temperature.

applied. The peak heights were used to estimate T_2. Because of the lack of data, no T_1 or n.O.e. effects could be taken into account. Therefore, no quantitative meaning can be given to the intensities. However, it is assumed that the ratios of intensities with respect to that of the peak for CH_3CO allow the melting behaviour to be monitored.

For analytical purposes, a ^{13}C-n.m.r. spectrum was obtained at 90°, using a 21.7 kHz spectral width and 5 Hz of line broadening, the accumulation of 53,000 scans, and a repetition time of 1 s digitised in a 16K memory to give a 1.33 Hz resolution. Chemical shifts were referred to external DSS (sodium 4,4-dimethyl-4-silapentanoate).

Light scattering. — Low-angle laser-light-scattering measurements were performed at 633 nm, using a Chromatix KMX6 photometer. The angular dependence of the intensity of scattered light from solutions of FS1 in 0.01M NaCl was obtained at 25° and 68° with a Fica 50 photogoniometer, using unpolarised light at 436 nm.

All solutions of xanthan were dialysed against NaCl (0.01 and 0.1M) and the outer dialysis solution was used for dilutions. The solutions were filtered through 0.45- and/or 0.22-μm Millipore membranes.

Increments in the specific refractive index. — Measurements of $(\delta n/\delta c)_\mu$ were performed at 436 and 633 nm, using Brice–Phoenix and Chromatix KMX16 differential refractometers, respectively, on dialysed solutions of xanthan.

Rate of relaxation of $^{23}Na^+$. — $^{23}Na^+$ relaxation rates as a function of temperature were obtained at 71.4 MHz, using a modified Bruker SXP spectrometer equipped with a 6.3-T superconducting magnet (Oxford Instruments). Low-field measurements were performed using a home-built spectrometer equipped with a 2.1-T electromagnet (Bruker) operating at 23.7 MHz. Some $^{23}Na^+$ relaxation-rate measurements were also performed at 105 and 132 MHz, using Bruker MSL 400 (9.4 T) and WM 500 (11.7 T) spectrometers, respectively.

Longitudinal-relaxation rates were obtained by the phase-alternated inversion–recovery method[33]. Transverse relaxation rates were determined by spin-echo experiments.

Relaxation rates at 23.7 and 71.4 MHz were obtained by collecting 100 data points, whereas only 30–70 data points were collected at higher field strengths. All data were fitted with a non-linear least-squares procedure to one exponential or a sum of two exponentials.

For the measurements at 71.4, 105, and 132 MHz, the temperature of the sample was controlled by an air thermostat (Bruker B-VT 1000). The probe of the low-field magnet was thermostated by circulating Fluorinert FC75 (3M Co), using a Braun Thermomix/Frigomix combination.

Samples of polymers for n.m.r. measurements were prepared in quartz n.m.r. tubes, except for the measurements at 105 and 132 MHz where glass n.m.r. tubes were used. The solutions of the polymers were degassed by shaking the n.m.r. tubes under N_2.

RELAXATION OF QUADRUPOLAR NUCLEI

For quadrupolar nuclei, the interaction of the nuclear quadrupole moment and

the fluctuating electric field gradient at the nucleus is generally by far the most efficient relaxation mechanism. The relaxation of longitudinal and transverse magnetisation is determined by the spectral density of the fluctuating interaction at multiples of the Larmor frequency.

For spin $I = 3/2$, expressions for the longitudinal and transverse relaxation have been derived by Hubbard[34]:

$$M_z(t) - M_0 = M_0(\cos\theta - 1)\,[1/5\,\exp(-R1_f t) + 4/5\,\exp(-R1_s t)] \quad (1)$$

$$M_{xy}(t) = M_0 \sin\theta\,[3/5\,\exp(-R2_f t) + 2/5\,\exp(-R2_s t)] \quad (2)$$

where:

$$R1_f = 2(eQ/h)^2 J(\omega) \quad (3)$$

$$R1_s = 2(eQ/h)^2 J(2\omega) \quad (4)$$

$$R2_f = (eQ/h)^2\,[J(0) + J(\omega)] \quad (5)$$

$$R2_s = (eQ/h)^2\,[J(\omega) + J(2\omega)] \quad (6)$$

where Q is the quadrupolar moment of the nucleus, ω is the Larmor frequency, e is the protonic charge, θ is the flip angle of the preparation pulse, and $J(\omega)$ is the spectral density.

If the Hamiltonian which governs the molecular motion is invariant under rotation, then the spectral density $J(\omega)$ is given by:

$$J(\omega) = 1/2 \int_{-\infty}^{+\infty} < F_0^{(2)}(t) \cdot F_0^{(2)}(t + \tau) > e^{i\omega\tau}\, d\tau \quad (7)$$

where $F_0 = 1/2V_{zz}$ and is the $m = 0$ component of the irreducible electric field gradient tensor F_m in the laboratory frame.

If the autocorrelation function of the electric field gradient decays exponentially, as is often assumed, the reduced spectral density $\tilde{J}(\omega)$ can be defined as

$$(eQ/h)^2 J(\omega) \equiv \pi^2/10 < (eqeQ/h)^2 > \tilde{J}(\omega) \equiv \pi^2/10 < \chi^2 > \tilde{J}(\omega) \quad (8)$$

where $\tilde{J}(\omega) = 2\tau_c/(1 + \omega^2\tau_c^2)$ and $< \chi^2 >$ is the mean square quadrupole coupling constant.

When the correlation time τ_c of the electric field gradient fluctuations is short with respect to the Larmor period, *i.e.*, when $\omega\tau_c << 1$, the extreme narrowing limit condition obtains. In this situation, $\tilde{J}(0) = \tilde{J}(\omega) = \tilde{J}(2\omega) = 2\tau_c$, and both longitudinal and transverse relaxation are exponential with rates $R1 = R2$.

For longer correlation times, *e.g.*, $\omega\tau_c \geq 0.1$, both relaxations are biexponential, although, in general, the longitudinal relaxation cannot be resolved into its two components because of the small amplitude of the fast component.

Nevertheless, as will be shown, it is possible to obtain reasonable estimates of $\tilde{J}(0)$, $\tilde{J}(\omega)$, and $\tilde{J}(2\omega)$, from which τ_c is obtained if the loss of correlation is assumed to be exponential. This assumption can be tested by measurements at different Larmor frequencies and over-determining the parameters in equation 8.

If the loss of correlation of the interaction Hamiltonian is due to different, independent processes, then equation *8* becomes:

$$(eQ/h)^2 J(\omega) = \pi^2/10 \sum_i < \chi_i^2 > \tilde{J}_i(\omega) \qquad (9)$$

As shown below, at least two correlation times, corresponding to a fast and a slow process, are necessary in order to describe the $^{23}Na^+$ relaxation rates in solutions of xanthan.

RESULTS

Characterisation of the samples of xanthan. — From elemental (N) analysis and absorbance measurements in the region 280–260 nm, a protein content of <2% for the samples of xanthan was estimated. Traces of nucleic acids were detected. From measurements of atomic absorption, no Ca^{2+} ions could be detected in ~1 g/L solutions of the xanthan ($Ca^{2+} < 1 \times 10^{-6}$ mol/L).

Table I contains data on the samples of xanthan. The contents of pyruvate and acetate groups were determined by ^{1}H-n.m.r. spectroscopy[32] on solutions in D_2O at 90° and by potentiometric titrations at room temperature. The 100-MHz ^{13}C-n.m.r. spectrum of a 2.6×10^{-2} monomol/L solution of FS3 in D_2O (see Fig. 1) shows a pattern of signals that is typical of a partially depyruvated xanthan[35,36].

The ^{13}C resonances of pyruvate and acetate C=O are at 177.53 and 176.64 p.p.m., respectively (the latter is superimposed on the C=O signal of the GlcA residue), and the

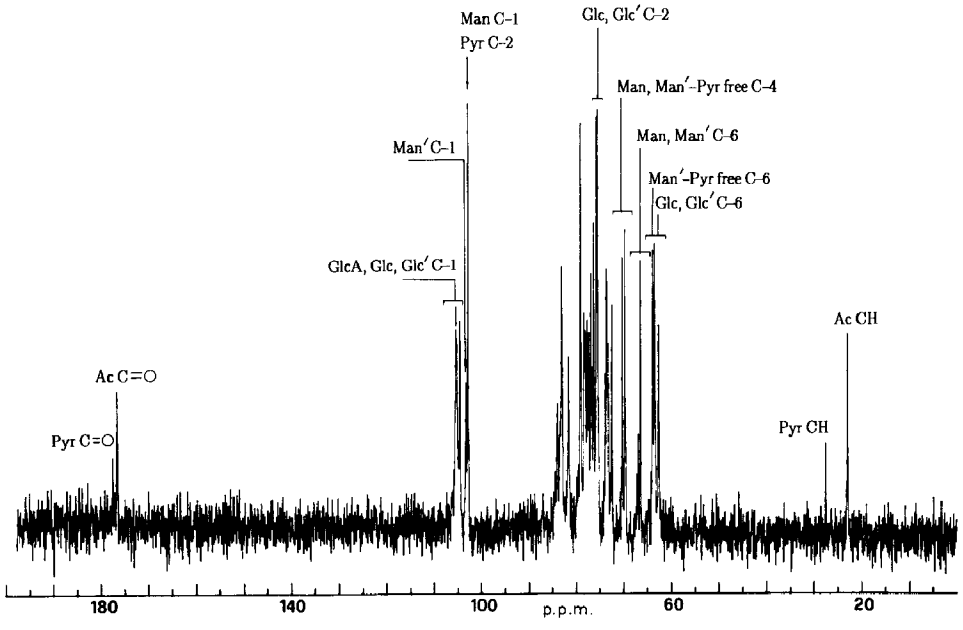

Fig. 1. ^{13}C-N.m.r. spectrum of a solution of 2.6×10^{-2} monomol/L FS3 in D_2O at 90° (5-Hz line broadening).

CH_3 signals at 27.5 and 22.84 p.p.m., respectively. Peaks assigned to C-6 of the Glc (62.6 p.p.m.) and Glc′ (63.48 p.p.m.) units, and to the Man′ (66.81 p.p.m.), Man (66.33 p.p.m.), and Man′ pyruvate-free (63.86 p.p.m.) residues[35,36] are well resolved, as are the peaks assigned to C-1 of Glc (105.2 p.p.m.), Glc′ (105.0 p.p.m.), GlcA (104.4 p.p.m.), Man′ (103.31 p.p.m.), and Man (102.8 p.p.m.), the latter being superimposed on the C-2 signal of the pyruvate substituent. The signals at 70.19 and 69.65 p.p.m. were assigned tentatively to C-4 of the Man and the non-pyruvated Man′ residues[37], respectively, whereas those at 75.6 and 75.37 p.p.m. are probably due to C-2 of the Glc and Glc′ residues, respectively, the latter showing a β-upfield shift due to the additional 3-substitution[37].

Dependence of optical activity on the concentration of the polymer and the temperature. — Measurements of optical activity have been used widely in studies of the conformational properties of solutions of xanthan. The sigmoidal change of $[\alpha]$ as a function of concentration of added ions has been interpreted normally as a conformational transition of the stretched coil to helix type. Figure 2 contains two sets of data on FS2: the △ symbols show the familiar conformational transition at constant concentration of polymer as a function of added salt[6], the ○ symbols represent $[\alpha]_{365}$ as a function of the concentration of the polymer without added salt, and *Ce* represents the total concentration of charge. The range of concentrations was chosen such that no gel was formed.

Comparison with the temperature-induced transition shown in Fig. 3 shows that the plateau values of $[\alpha]_{365}$ for FS2 are the same, which supports the conclusion that the ○ symbols in Fig. 3 show a conformational transition induced by change in the concentration of the polymer.

For comparison, $[\alpha]_{365}$ values obtained from 1.0–2.0 $\times$ 10^{-3} monomol/L solutions of FS3, FS2, and FS1 in 0.01M NaCl are reported (filled symbols in Fig. 3).

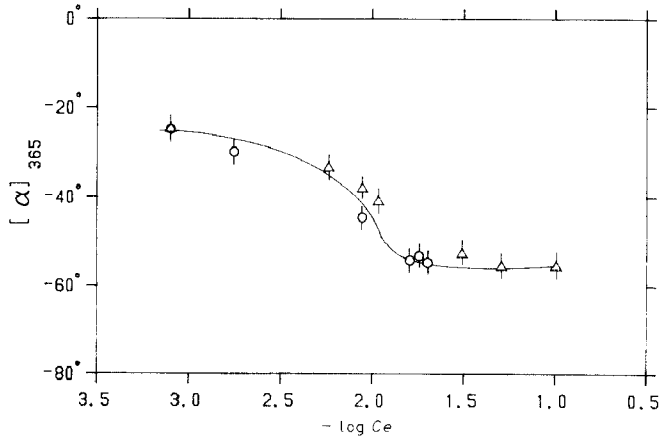

Fig. 2. Dependence of optical activity on the − log of the total molar charge concentration (*Ce*) for solutions of FS2 at 25° and 365 nm: ○, solutions with no added salt; △, solutions in the presence of added NaCl at a constant *Cp* (5.3 $\times$ 10^{-4} monomol/L).

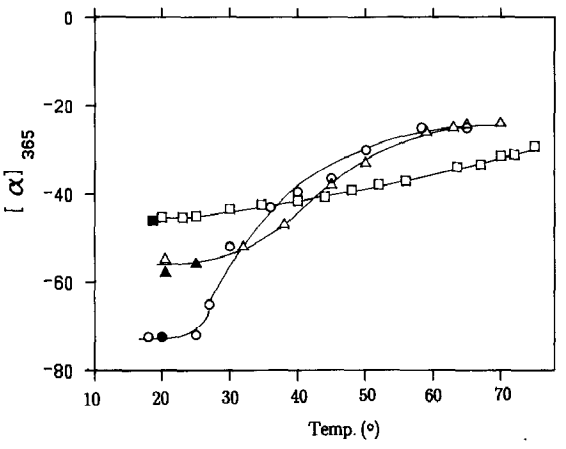

Fig. 3. Temperature dependence of optical activity of solutions of ○, FS1 (*Cp* 4.9 × 10^{-3} monomol/L); △, FS2 (*Cp* 1.28 × 10^{-2} monomol/L); □, FS3 (*Cp* 2.6 × 10^{-2} monomol/L in D_2O–H_2O (1:1). Filled symbols refer to more dilute solutions (1.0–2.0 × 10^{-3} monomol/L) with added salt (0.01M NaCl).

The melting process showed hysteresis, the magnitude of which was dependent upon the cooling rate. Steps of 2–5° during the cooling process could take 24 h to stabilise.

No significant change of the molecular weight was detected for a solution of FS1 in 0.01M NaCl by light-scattering measurements performed at 25° and 68°. This result confirms previous findings[12] that the conformational transition monitored by changes in optical activity does not involve the full dissociation of dimers.

^{13}C-N.m.r. spectra as a function of temperature. — A sequence of spectra of a solution of 2.6 × 10^{-2} monomol/L of FS3 in H_2O–D_2O (1:1) as a function of temperature is depicted in Fig. 4 A–C. A line broadening of 50 Hz was applied, and no quantitative significance can be given to the intensities. Therefore, the peak for CH_3CO, which shows the smallest temperature dependence, was used as an internal reference.

As expected, all intensities increased with increase in the temperature. Up to 59°, which is above the transition temperature, the pyruvate Me signal is stronger than that of acetate Me, although the content of acetate is nearly twice that of pyruvate. Below 59°, the signal from C-6 of Glc and Glc′ (overlapping C-6 of Man′-pyruvate free) is broader and less developed than that of C-6 of Man and Man′. The latter signal is well above the noise level at 50°. Likewise, the C-1 resonances of Glc, Glc′, and GlcA are broader than those of C-1 of Man and Man′, and of C-2 of Pyr, and develop at higher temperature. Figure 5 summarises the relative intensities as a function of temperature, compared to that of the acetate Me signal. When the samples were cooled and the spectra run again at 90°, a decrease or even a lack of the pyruvate Me signal was observed.

Temperature dependence of the rates of relaxation of $^{23}Na^+$. — $^{23}Na^+$ and ^{17}O relaxation measurements obtained at 6.3 T (71.4 and 36.6 MHz, respectively) for an aqueous salt-free 1.2 × 10^{-2} monomol/L solution of FS2 are reported in Fig. 6 as a

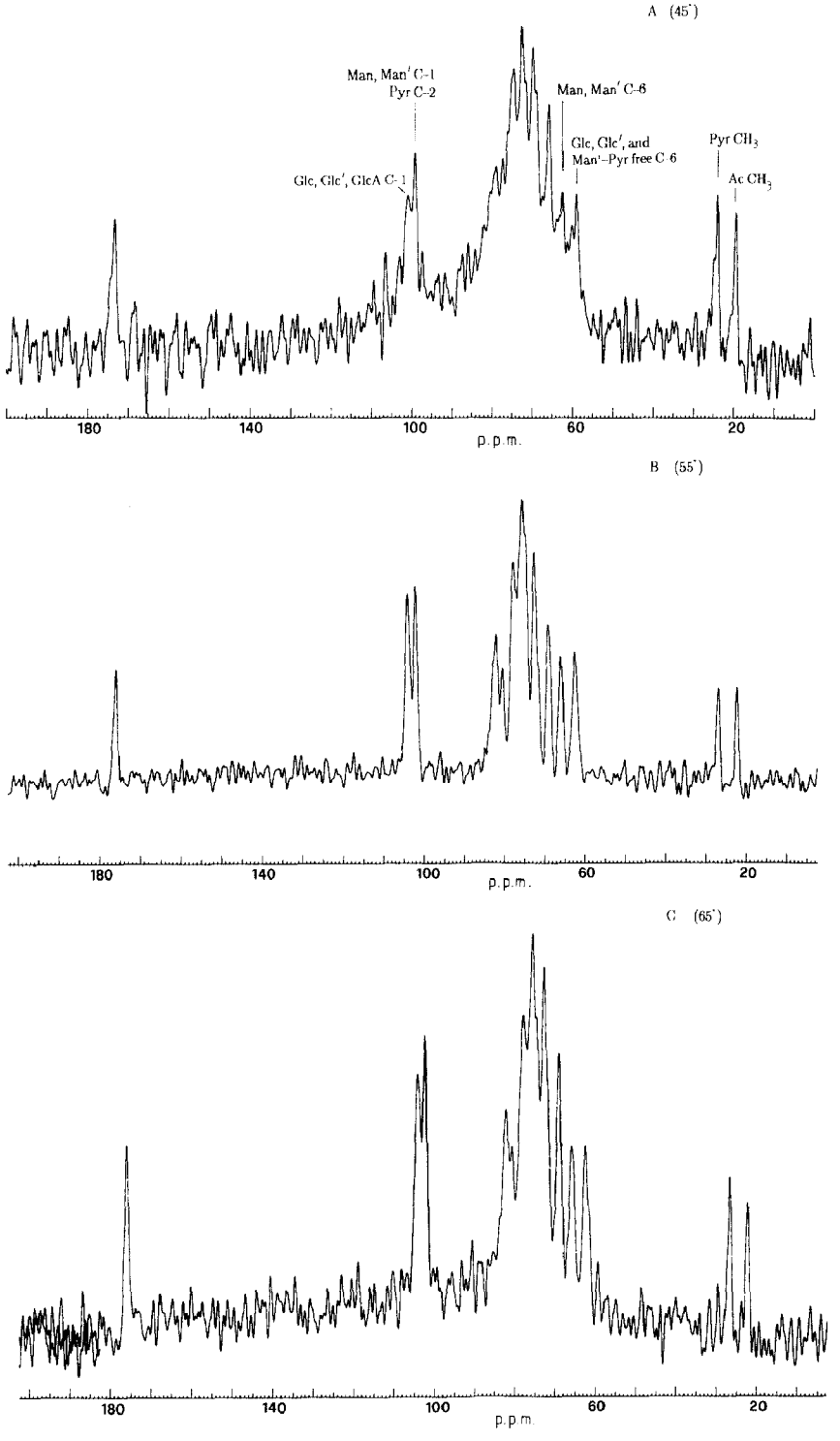

Fig. 4. ^{13}C-N.m.r. spectra of a 2.6 × 10^{-2} monomol/L solution of FS3 in D_2O–H_2O (1:1) as a function of temperature (50-Hz line broadening).

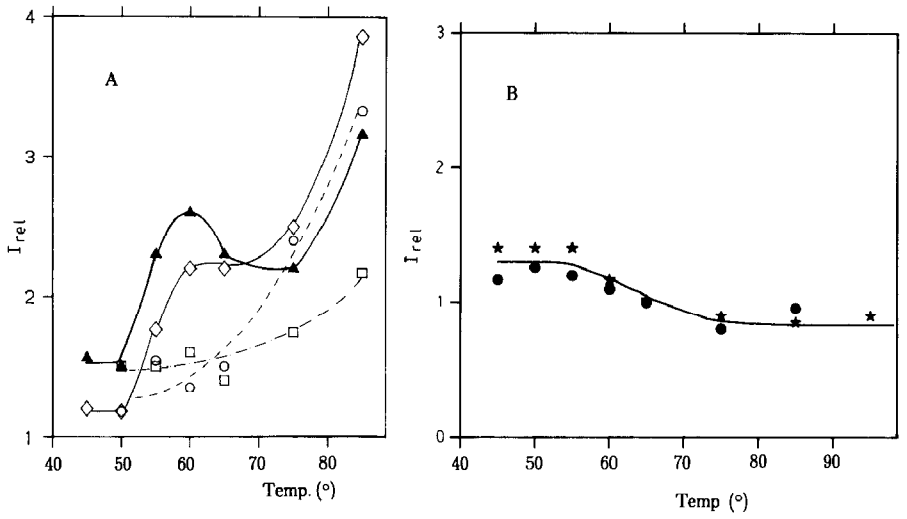

Fig. 5. A, Peak amplitudes relative to that of the acetate Me signal (□, Man and Man' C-6:Ac Me; ▲, Man and Man' C-1, Pyr C-2:Ac Me; ○ Glc and Glc' C-6:Ac Me;◇, Glc, Glc', and GlcA C-1:Ac Me); B, temperature dependence of signal intensity ratios [■, Pyr Me:Ac Me; ★, (Man C-1, Man' C-1, Pyr C-2):(Glc, Glc', and GlcA C-1)].

function of temperature. Similar curves were obtained for FS1 and FS3 (data not shown).

Figure 6 shows that the extreme narrowing limit condition does not apply for ^{23}Na relaxation over the entire range of temperatures. As found for other synthetic and natural polyelectrolytes[25,26], biexponential transverse relaxation with $R2_f > R1$ and $R2_s > R1$ is found. Upon cooling, the relaxation rates were reversible except for the $R2_f$

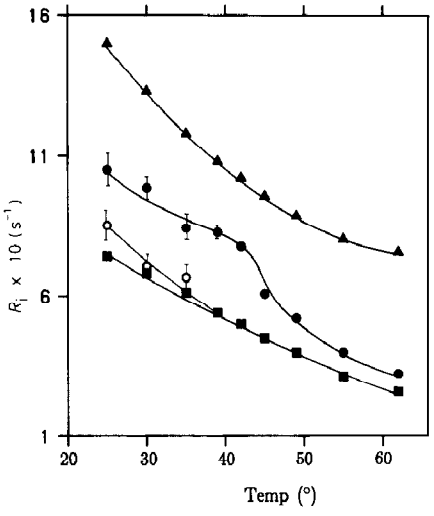

Fig. 6. Temperature dependence of ^{23}Na and ^{17}O relaxation rates of a 1.2×10^{-2} monomol/L solution of FS2 at 71.41 MHz: ▲, $R1$ ^{17}O; ●, $R2_f$ ^{23}Na; ○, $R2_s$ ^{23}Na; ■, $R1$ ^{23}Na.

values which fell in the region 37–45°. In this range, the value of $R2_f$ on cooling did not reach those before heating.

Table II contains relaxation rates in the temperature range 25–45° for a salt-free 1.8×10^{-2} monomol/L solution of FS2 measured at different field strengths.

Spectral densities at the different frequencies have been obtained using equations *3–6* and the approximation $R1 \approx [4/5R1_s + 1/5R1_f]$. Using an iterative procedure, the spectral densities were adjusted until the experimental relaxation rates in Table II were reproduced to within 5–8% (see Fig. 7). As found earlier[25,26], the high frequency tail of the spectral density shows that a single correlation time does not suffice to describe the modulation process of the electric-field gradients.

In order to fit the experimental values reported in Fig. 7, a Lorentzian and a constant were needed. The latter represents the spectral density due to at least one process with a short correlation time τ_2:

$$(eQ/h)^2 J(\omega) = \pi^2/5 < \chi_1^2 > \frac{\tau_1}{1+\omega^2\tau_1^2} + \pi^2/5 < \chi_2^2 > \tau_2 \qquad (10)$$

Table III contains the spectral density parameters τ_1, $<\chi_1^2>$, and $<\chi_2^2>\tau_2$ obtained.

DISCUSSION

The optical activity data in Figs. 2 and 3 clearly show the occurrence of a

TABLE II

^{23}Na relaxation rates in a 1.8×10^{-2} monomol/L solution of FS2

Temp. (°)	*223.8 MHz*			*71.4 MHz*			*105.8 MHz*			*132 MHz*		
	$R1$	$R2_s$	$R2_f$	$R1$	$R2_s$	$R2_f$	$R1$	$R2_s$	$R2_f$	$R1$	$R2_s$	$R2_f$
25	101	106	156	81	84	132	73	—	—	74	74	120
33	81	81	120	68	68	103	—	—	—	68	68	90
50	50	50	62	45	45	60	—	—	—	—	—	—
55	41	41	54	38	38	51	—	—	—	36	40	40

TABLE III

Spectral density parameters from fitting experimental $(eQ/h)^2 J(\omega)$ values with equation *10* (curves of Fig. 7)

Temp. (°)	τ_1 *(ns)*	$<\chi_1^2>^{1/2}$ *(kHz)*	$<\chi_2^2>\tau_2$ *(Hz)*
25	6.8	61.6	18.74
33	6.0	52.45	16.2
50	4.7	35.16	11.15
55	3.9	32.4	9.12

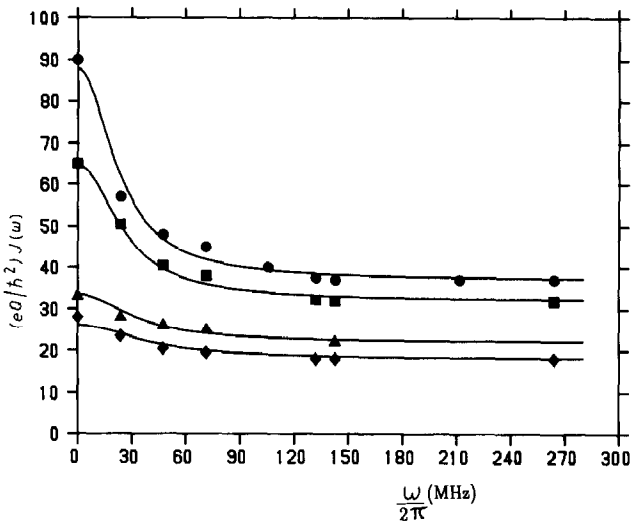

Fig. 7. Frequency dependence of experimental $(eQ/h)^2J(\omega)$ values for a 1.8×10^{-2} monomol/L solution of FS2 as a function of temperature. Solid lines represent the calculated spectral densities (see text): ●, 25°; ■, 33°; ▲, 50°; ◆, 55°.

conformational transition, as a function of both temperature and ionic strength. In accordance with the stabilising effect of the concentration of the polymer on the ordered structure (see Fig. 2), the sigmoidal parts of the melting curves shift to higher temperatures with increase of the concentration from FS1 to FS3 in Fig. 3. The low-temperature results in Fig. 3 show that the extent of ordering decreases with decrease in molecular weight from FS1 to FS3 even though the concentration is higher for the lower molecular weights. Thus, the molecular weight has an important influence on the stability of the ordered conformation of xanthan in the region 5×10^5–1.8×10^6 studied. The results in Fig. 3 show that a molecular weight of 10^5 is probably close to the smallest value for the occurrence of the low-temperature conformation at 22°. In previous work, an influence of the molecular weight on the stability was seen in the enthalpy of protonation[8] and in the melting temperature[38]. The dependence of the optical activity on the molecular weight was reported[15] only for samples of xanthan with molecular weights below 10^5. The high- and low-temperature plateau values of the optical activity depended on the molecular weights of the samples, whereas, in the present work, only the low-temperature plateau shows this dependence. Clearly, more work needs to be done, especially with respect to the detailed effect of the sonication procedure, before a detailed description can be constructed. The concentrations for the n.m.r. work were chosen so as to ensure that the ordered conformation was present at the lowest temperature in any series of measurements.

The ^{13}C-n.m.r. data demonstrate a difference in behaviour between the side chains and the main chain as a function of temperature. In the premelting range, the side-chain signals tend to be larger than those of the main chain. In Fig. 5, the peak amplitudes relative to that of the acetate Me group are displayed as a function of temperature. In the

melting range, the amplitude of the C-1 signals especially show a large initial increase followed, at a higher temperature, by those of C-6. If the change of the peak intensity is tentatively attributed to a change in T_2 values, these results indicate an important initial increase of the mobility of C-1 with increase in temperature. This effect is to be expected because conformational changes arise through rotations about the glycosidic linkage in which the C-1 is involved. The behaviour of the side-chain signal indicates that a considerable side-chain mobility is established before an important increase in the mobility of the backbone occurs.

The ^{23}Na and ^{17}O relaxation rates are collected in Fig. 6 and Tables II and III. The relaxation behaviour of the counter-ion changes on melting the ordered conformation of xanthan. In the transition region, the long correlation time decreases, which leads to practically exponential transverse and longitudinal relaxation. In contrast to the relaxation behaviour in DNA[25], no equality of T_1 and T_2 is reached in or just above the melting range indicated by the optical rotation. This finding means that even the high-temperature conformation generates correlation times in the ns range for the electric-field gradients observed by the Na nuclei. A possible explanation may be the persistence of ordered regions in the xanthan molecules after the melting of the original ordered conformation. If, in view of the constancy of the molecular weight, the transition is pictured as the unfolding of a double helix to yield still-connected strands, the ^{23}Na results are consistent with the existence of remaining helical sequences of a single or double stranded nature.

From the value of $<\chi_2^2>\tau_2$ at 25° in Table III, it is seen that the high frequency contribution to the ^{23}Na relaxation is 75 s^{-1}, which is considerably larger than that (17 s^{-1}) obtained for a dilute solution of simple electrolyte. In the latter solutions, the ^{23}Na relaxation is due to the time-dependent coupling of the nuclear quadrupole with the electric-field gradient from the surrounding water dipoles. The same mechanism is expected to give a high-frequency contribution to the counter-ion relaxation in solutions of xanthan. In this context, it is of interest to note that, again at 25°, the ^{17}O $R1$ is increased from 140 s^{-1} for a dilute electrolyte solution to 152 s^{-1} in the solutions of xanthan.

Clearly, the rate of reorientation of part of the water molecules is diminished and it is to be expected that the water molecules near the xanthan polymer are involved. As the distribution of the counter-ions in solution is biased towards a larger concentration near the charged polymers, the observed reduction of the average mobility of the water molecules should be amplified in the high-frequency contribution to the ^{23}Na rate. The present results are consistent with this reasoning. Further work should yield a more detailed picture of the influence of the xanthan molecules on the microdynamical properties of the counter-ions and the water molecules.

ACKNOWLEDGMENT

We thank Professor M. Mandel for stimulating discussions.

REFERENCES

1 G. Cuvelier and B. Launay, *Carbohydr. Polym.*, 6 (1986) 321–333.
2 R. K. Richardson and S. B. Ross-Murphy, *Int. J. Biol. Macromol.*, 9 (1987) 257–264.
3 J. F. Kennedy and I. J. Bradshaw, *Prog. Ind. Microbiol.*, 19 (1984) 319–371.
4 P.-E. Jansson, L. Kenne, and B. Lindberg, *Carbohydr. Res.*, 45 (1975) 275–282.
5 G. Holzwart, *Biochemistry*, 15 (1976) 4333–4339.
6 S. Paoletti, A. Cesaro, and F. Delben, *Carbohydr. Res.*, 123 (1983) 173–178.
7 M. Milas and M. Rinaudo, *Carbohydr. Res.*, 158 (1986) 194–204.
8 V. Crescenzi, M. Dentini, and L. Pietrelli, *Period. Biol.*, 83 (1981) 125–128.
9 E. R. Morris, D. A. Rees, G. Young, M. D. Walkinshaw, and A. Darke, *J. Mol. Biol.*, 110 (1977) 1–16.
10 I. T. Norton, D. M. Goodall, E. R. Morris, and D. A. Rees, *J. Chem. Soc., Chem. Commun.*, (1980) 545–547.
11 G. Muller, M. Anrhourrache, J. Lecourtier, and G. Chauveteau, *Int. J. Biol. Macromol.*, 8 (1986) 167–172.
12 W. Liu, T. Sato, T. Norisuye, and H. Fujita, *Carbohydr. Res.*, 160 (1987) 267–281.
13 J. Lecourtier, G. Chauveteau, and G. Muller, *Int. J. Biol. Macromol.*, 8 (1986) 306–310.
14 W. Liu and T. Norisuye, *Biopolymers*, 27 (1988) 1641–1654.
15 W. Liu and T. Norisuye, *Int. J. Biol. Macromol.*, 10 (1988) 44–50.
16 G. Gravanis, M. Milas, M. Rinaudo, and B. Tinland, *Carbohydr. Res.*, 160 (1987) 259–265.
17 T. Sato, T. Norisuye, and H. Fujita, *Polym. J.*, 16 (1984) 341–350.
18 T. Sato, T. Norisuye, and H. Fujita, *Macromolecules*, 17 (1984) 2629–2700.
19 G. Paradossi and D. A. Brant, *Macromolecules*, 15 (1982) 874–879.
20 B. T. Stokke, A. Elgsaeter, and O. Smidsröd, *Int. J. Biol. Macromol.*, 8 (1986) 217–225.
21 L. Hacche, G. E. Washington, and D. A. Brant, *Macromolecules*, 20 (1987) 2179–2187.
22 J. J. van der Klink, L. H. Zuiderweg, and J. C. Leyte, *J. Chem. Phys.*, 60 (1974) 2391–2399.
23 C. J. M. van Rijn, A. J. Maat, J. de Bleijser, and J. C. Leyte, *J. Phys. Chem.*, 93 (1989) 5284–5291.
24 S. Paoletti, F. Delben, A. Cesaro, and H. Grasdalen, *Macromolecules*, 18 (1985) 1834–1841.
25 L. van Dijk, M. L. H. Gruwel, W. Jesse, J. de Bleijser, and J. C. Leyte, *Biopolymers*, 26 (1987) 261–284.
26 C. W. R. Mulder, J. de Bleijser, and J. C. Leyte, *Chem. Phys. Lett.*, 69 (1980) 354–358.
27 H. Gustavsson, G. Siegel, B. Lindman, and L.-A. Fransson, *FEBS Lett.*, 86 (1978) 127–130.
28 B. Halle, H. Wennerström, and L. J. Piculell, *J. Phys. Chem.*, 88 (1984) 2482–2494.
29 H. Gustavsson, G. Siegel, B. Lindman, and L.-A. Fransson, *Biochim. Biophys. Acta*, 677 (1981) 23–31.
30 (*a*) H. Grasdalen and B. J. Kvam, *Macromolecules*, 19 (1986) 1913–1920; (*b*) B. J. Kvam and H. Grasdalen, *ibid.*, 22 (1989) 3919–3928.
31 L. Piculell and B. Lindman, *Biopolymers*, 23 (1984) 1683–1699.
32 J. F. Kennedy, D. L. Stevenson, C. A. White, M. S. Tolly, and I. J. Bradshaw, *Br. Polym. J.*, 16 (1984) 5–10.
33 D. E. Demco, P. van Hecke, and J. S. Waugh, *J. Magn. Reson.*, 16 (1974) 467–470.
34 P. S. Hubbard, *J. Chem. Phys.*, 53 (1970) 985–987.
35 D. Horton, O. Mols, and Z. Walaszek, *Carbohydr. Res.*, 141 (1985) 340–346.
36 M. Rinaudo, M. Milas, F. Lambert, and M. Vincendom, *Macromolecules*, 16 (1983) 816–819.
37 P. A. J. Gorin, *Adv. Carbohydr. Chem. Biochem.*, 38 (1981) 13–104.
38 M. Milas and M. Rinaudo, *ACS Symp. Ser.*, 150 (1981) 25–30.